JOURNAL OF GEOPHYSICAL RESEARCH, VOL. 101, NO. A4, PAGES 7737–7747, APRIL 1, 1996

Magnetic storms and magnetotail currents

I. I. Alexeev, E. S. Belenkaya, and V. V. Kalegaev

Institute of Nuclear Physics, Moscow State University, Moscow, Russia

Y. I. Feldstein

Institute of Terrestrial Magnetism, Ionosphere and the Radiowave Propagation
Troitsk, Moscow Region, Russia

A. Grafe

GeoResearch Center Potsdam, Adolf Schmidt Observatory, Niemegk, Germany

Abstract. The magnetospheric magnetic field is highly time-dependent and may have explosive changes (magnetospheric substorms and geomagnetic storms) accompanied by significant energy input into the magnetosphere. However, the existing stationary magnetospheric models can not simulate the magnetosphere for disturbed conditions associated with the most interesting magnetospheric physics events (intensive auroras, particle injection in the inner magnetosphere, and precipitations at the high latitudes, etc.). We propose a method for constructing a nonstationary model of the magnetospheric magnetic field, which enables us to describe the magnetosphere during the disturbances. The dynamic changes of the magnetosphere will be represented as a sequence of quasi-stationary states. The relative contributions to the Dst index by various sources of magnetospheric magnetic field are considered using a dynamic model of the Earth's magnetosphere. The calculated magnetic field is obtained by using the solar wind and geomagnetic activity empirical data of the magnetic storm of March 23–24, 1969 and the magnetic disturbance of July 24–26, 1986. The main emphasis is on the current system of the magnetospheric tail, the variations of which enable a description of the fast changes of Dst.

1. Introduction

When the Dst index of the geomagnetic field during geomagnetic storm is analyzed, it is apparent that in addition to an observed smooth variation of Dst with a characteristic time of $\simeq$10 hours, as a rule, rapid variations with a characteristic time of $\simeq$1 hour are also detected. However, opinions about the cause of these variations are rather contradictory at present [*Feldstein,* 1992; *Grafe and Best,* 1966; *Tinsley and Akasofu,* 1982; *Pisarsky et al.,* 1986; *Grafe,* 1988; *Gonzales et al.,* 1990]. Measurements of the spectrum of energies (1–300 KeV/q) in the ring current region ($L \sim$ 3–6) show that the main mechanism of losses is a charge exchange with the exosphere neutrals (see e.g., the AMPTE data by *Kistler et al.* [1989]). *Fok et al.* [1993] describe the influence of the Coulomb collisions with plasmaspheric ions on the ring current ions lifetime. Another ring current loss process is pitch angle diffusion driven by ion-cyclotron resonance [*Eather and Carovillano,* 1971]. The typical time of change of ring current ions flux determined by these loss processes is about 10 hours [see e.g., *Fok et al.,* 1993; *Gonzales et al.,* 1994], and it is possible to explain smooth variations of Dst index by these processes. However, it is not possible to explain rapid (about 1 hour) changes in Dst index during the recovery phase by similar intensity variation of the ring current particles. While an increase of the Dst absolute value can be due to particle injection, a similar rapid decrease of disturbance can hardly be associated with an abrupt drop of intensity resulting from particle losses due to the precipitation or charge exchange. This fact makes it reasonable to raise again the question of possible sources of Dst index, other than the ring current particles. A current system of the magnetospheric tail [*Alexeev et al.,* 1975] and currents at the magnetopause [*Alexeev,* 1978] are the most likely candidates. Therefore following *Maltsev* [1991], we shall deal with the influence of tail current system on the Dst index geomagnetic field.

Paper number 95JA03509.
0148-0227/96/95JA-03509$05.00

2. Model

Relative contributions to the Dst index by various sources of magnetic field (the ring current, currents on the magnetopause, and the current system of the magnetospheric tail) may be estimated using a dynamic magnetospheric model. This approach is valid if we neglect transition processes with

characteristic time less than the Alfven wave propagation time along magnetospheric field lines (that is, about 10 min). Here variations of the magnetospheric field with time scale more than 1 hour will be described. These time variations will be characterized by modification of the magnetosphere parameters. To calculate a modeled magnetospheric field, use was made of a paraboloid magnetospheric model [*Alexeev*, 1978]:

$$\mathbf{B}_m = \mathbf{B}_d(\psi) + \mathbf{B}_{sd}(\psi, R_1) + \mathbf{B}_t(\psi, R_1, R_2, \Phi_\infty) + \mathbf{B}_r(\psi, b_r) + \mathbf{B}_{sr}(\psi, R_1, b_r)\,. \quad (1)$$

Here $\mathbf{B}_d$ is the dipole field; $\mathbf{B}_{sd}$ is the field of currents on the magnetopause screening the dipole field; $\mathbf{B}_t$ is the field of the magnetospheric tail current system (cross-tail currents and closure magnetopause currents); $\mathbf{B}_r$ is the field of ring current calculated in terms of the model similar to the Tsyganenko one [*Tsyganenko and Usmanov*, 1982], but the ring current terminates at a fixed distance, and beyond this distance, $\mathbf{B}_r$ is proportional to the dipole field; $\mathbf{B}_{sr}$ is the field of currents on the magnetopause screening the ring current field. In the total field $\mathbf{B}_m$ (equation (1)) the interplanetary magnetic field penetrating into the magnetosphere is not presented, as its value is rather small [see *Alexeev*, 1986].

The dynamic model depends on five time-dependent input parameters: ψ (dipole tilt angle); R_1 (magnetopause subsolar distance); R_2 (the distance to the earthward edge of the current sheet in the magnetospheric tail); Φ_∞ (the tail lobe magnetic flux which defines the intensity of the magnetospheric tail current); and b_r (the ring current magnetic field intensity at the Earth's equator).

We will test model calculations by comparison with observational values of the Dst index. The Dst index presents a symmetric part of the magnetic field disturbance at the Earth's equator. Latitudinal component of the magnetic field of the region 1 field-aligned currents has opposite signs on the dayside and nightside in the equatorial plane. We will not study an asymmetric part of magnetic disturbance hence the subject of the field-aligned currents will not be included in our consideration. For the same reason the asymmetric magnetic field of the partial ring current, of the middle-latitude ionospheric currents, etc., will be omitted too. A more detail discussion of this topic is included in section 5.

Although our model current systems cannot be claimed as a unique set of currents for describing the observations, they represent a best fit solution which is consistent with general knowledge of the behavior of magnetospheric currents.

3. Calculations

Let us calculate the magnetospheric magnetic field using empirical data of the solar wind density and velocity and the auroral and geomagnetic activity (AL index, Dst, and the latitudinal location of the westward electrojet maximum at midnight). To compare the obtained model results with the onground measurements, we calculate

$$\Delta\mathbf{B}(t) = \mathbf{B}_m(t) - \mathbf{B}_d = \mathbf{B}_{sd} + \mathbf{B}_t + \mathbf{B}_r + \mathbf{B}_{sr}\,. \quad (2)$$

The input parameters of the dynamic model are obtained from the empirical data.

3.1. Geomagnetic Dipole Tilt Angle

The geomagnetic dipole tilt angle ψ is obtained from

$$\sin\psi = -\sin\beta\cos\alpha_1 + \cos\beta\sin\alpha_1\cos\varphi_m \quad (3)$$

where $\alpha_1 = 11.43°$ is the angle between the Earth's axis and the geodipole moment, β is the declination of the Sun ($\sin\beta = \sin\alpha_2\cos\varphi_{se}$), $\alpha_2 = 23.5°$ is the angle between the Earth's axis and the normal to the ecliptic plane, $\varphi_{se} = 0.9856263(172 - I_{\mathrm{day}})$ is the angle between the Sun-Earth line and the projection of the Earth's axis on the ecliptic plane, I_{day} is the day's number, and $\varphi_m = \mathrm{UT}\ 15° - 69.76°$ is the angle between the noon-midnight and north magnetic pole meridians, UT is the universal time in hours.

The tilt angle ψ is the single model parameter which has explicit time dependence. For calculation of other parameters it is necessary to construct more or less complex submodels. Model parameters are determined from observational data.

3.2. Magnetopause Subsolar Distance

The distance from the Earth to subsolar point at the magnetopause R_1 is the main parameter which determines the scale of the magnetosphere. This value is usually calculated from the balance between dynamic and magnetic pressures using data of the solar wind velocity v and density n

$$R_1 = 100/(nv^2)^{1/6} \quad (4)$$

(R_1 is in R_E ; n is in cm^{-3} ; and v is in km/s).

According to *Aubry et al.* [1970], *Fairfield* [1971], and *Kovner and Feldstein* [1973] the subsolar distance depends not only on the dynamic pressure of solar wind but also on the interplanetary magnetic field (IMF) B_z component. An enhancement of the southward component of IMF results in the decreasing of subsolar distance. The subsolar distance R_1 was calculated by us based on the result of *Roelof and Sibeck* [1993].

3.3. Distance to the Earthward Edge of the Current Sheet

The geotail current system consists of the dawn-dusk directed neutral sheet currents as well as of the magnetopause closure currents [*Alexeev et al.*, 1975]. The magnetic field of these currents depends on two spatial parameters: the subsolar distance R_1 and the distance to the earthward edge of the current sheet in the magnetospheric tail R_2. The value of R_2 will be calculated as

$$R_2 = 1/\cos^2\varphi_k\,, \quad (5)$$

where R_2 is in R_E and φ_k is the latitude of the maximum of the midnight auroral electrojet.

Two assumptions are used in (5). First of all, use is made of the dipolar relation between the equatorial distance to the field line and the latitude of its intersection with the Earth's

surface. We suppose that magnetic field lines are quasi-dipolar type earthward of the inner edge of the geotail current sheet [*Pullkinen,* 1991]. Second, we suppose that the inner edge of the tail current sheet is mapped to the electrojet maximum. As one can see in section 4.2 and in Figure 6, there is a good agreement between the values of φ_k obtained from the observation data (European Incoherent Scatter (EISCAT) magnetometer chain data) and calculated latitude of the equatorward auroral oval boundary.

3.4. Tail Lobe Magnetic Flux

We will define the intensity of the magnetospheric tail current by the value of the tail lobe magnetic flux Φ_∞. The magnetic flux in the geotail lobe approaches a constant as one moves away from the Earth. As was discussed by *Rostoker and Skone* [1993], the increasing area of the lobe cross section is balanced by an appropriate decrease in the tail lobe field magnitude. The tail lobe flux Φ_∞ is calculated as

$$\Phi_\infty = \lim_{x\to-\infty} \int_S \mathbf{B}_t d\mathbf{s}\,, \tag{6}$$

where $\mathbf{B}_t$ is the tail magnetic field and S is the tail lobe cross section. For the paraboloid model [*Alexeev et al,* 1975; *Alexeev,* 1978], Φ_∞ will be defined by R_1, R_2 and b_t, where b_t is the strength of the tail current magnetic field at the earthward edge of the tail current sheet. The value b_t is proportional to the maximum magnitude of the tail current density. We have (see Appendix) :

$$\Phi_\infty = b_t \frac{\pi R_1^2}{2}\sqrt{\frac{2R_2}{R_1}+1}\,. \tag{7}$$

For description of the disturbed tail current system, we will calculate Φ_∞ as sum

$$\Phi_\infty = \Phi_0 + \Phi_s\,, \tag{8}$$

where Φ_0 is the undisturbed (quiet) tail lobe magnetic flux and Φ_s is the disturbed time-dependent lobe magnetic flux, which is associated with enhancement of tail current system during disturbances.

For values characteristic of an undisturbed magnetosphere, $R_1 = 10\ R_E$, $R_2 = 7\ R_E$, $b_t = 40$ nT, we obtain from (7) the quiet magnetic flux through the tail lobe, $\Phi_0 = 3.7\ 10^8$ Wb [*Stern and Alexeev,* 1988]. From (7) we can thus determine adiabatic change of b_{t0} by the known R_1 and R_2, where b_{t0} is the field strength near the earthward edge of the quiet tail current

$$b_{t0} = \frac{2\Phi_0}{\pi R_1^2}\sqrt{R_1/(2R_2+R_1)}\,. \tag{9}$$

Using R_1 and R_2 calculated from (4) and (5), we find that b_{t0} varies in the range of 40–70 nT during the disturbance under consideration.

During disturbed times when substorm activity occurs, the tail lobe flux includes an additional term. This term is defined by (7) with $b_t = b_{ts}$, where b_{ts} is an enhancement of the field strength near the earthward edge of the tail current sheet. This value is calculated from the AL index:

$$b_{ts} = -k(AL)\,. \tag{10}$$

It is assumed in (10) that the additional disturbed tail current is proportional to the westward electrojet intensity. This fact was recognized by *Lui et al.* [1992] based on AMPTE/CCE data [see *Lui et al.,* 1992, Figure 12c]. *Lui et al.* [1992] found that the amount of tail current buildup prior to dipolarization was related to the subsequent strength of the substorm westward electrojet.

The numerical coefficient k in (10) was calculated by *Alexeev et al.* [1992] from the fact that the westward electrojet is the ionospheric part of the substorm current wedge. The ratio of the area of the ionospheric cross section of the substorms current wedge to the area of the tail cross section of the same current loop gave us $k \cong 1/7$ for $R = 6\ R_E$. A similar relation was obtained by *Lopez and von Rosenvinge* [1993] from statistical analysis of the correlation between field perturbation (δH) directly below the westward electrojet and B_p (deviation from the dipole field at the earthward boundary of the tail current sheet) during substorm:

$$\delta H = 7.2B_p - 188\,. \tag{11}$$

Here $(-\delta H)$ is the same as the AL index because δH is the perturbation of the H component at Poste de la Baleine which was the reporting station during the cases studied [*Lopez and von Rosenvinge,* 1993].

The formula (10) was supported by the results of *Kaufmann* [1987]. He used the observations of tail-like magnetic field patterns in the geosynchronous region during disturbances. To explain the field value $b_t \cong 180$ nT [*Kaufmann,* 1987], it is necessary to use the value of $k \simeq 1/7$.

It is clear to us that (10) does not take into account the total dynamics of the cross-tail currents. Perturbation of this current system has complex features with several different time scales and space scales. However, our study is concentrated on the main question about the strength of the tail current contribution to the magnetic field on the Earth's surface. A more precise equation instead of (10) which includes more parameters will lead us to a more complex model and will make our results less explicit. For this reason we started from the simple relation (10).

A similar modification of the geomagnetic tail field b_t was proposed by *Pullkinen et al.* [1991]. The increased level of the tail flux during the magnetospheric substorm was modeled by the transformation of b_t into $(1+f)b_t$, where f is the constant determined from empirical data.

3.5. Ring Current Intensity

The Dessler-Parker-Scopke relation

$$b_r = -\frac{2}{3}B_0\frac{\varepsilon_r}{\varepsilon_d} \tag{12}$$

associates the ring current field in the Earth's center b_r with the total ring current particles energy ε_r [*Akasofu and Chapman,* 1972]. Here B_0 is the dipole field at the Earth's equa-

tor, and $\varepsilon_d = \frac{1}{3}B_0M$ is the dipole field energy (M is the geodipole magnetic moment). According to this relation, one need not use a specific geometry of the ring current when considering the Dst index. We will use the ring current field model with fixed spatial parameters (the geocentric distances to the ring current maximum and to the ring current outer boundary).

The magnitude of the ring current magnetic field b_r depends on three parameters: t_0 is the moment of injection, τ_0 represents the characteristic decay time of the ring current, and b_{r0} is the magnetic field corresponding to the current maximum during the disturbance. Before the moment t_0, b_r (and ε_r as one can see from (12)) is assumed to be zero. After t_0, b_r is described by the formula

$$b_r = \frac{1}{\tau_0} b_{r0}(t - t_0)\exp\{(t - t_0 - \tau_0)/\tau_0\}. \qquad (13)$$

This relation describes the usual time dependence of the energy $\varepsilon_r(t)$ (see review of *Gonzalez et al.* [1994]). It represents both the single-particle injection into the ring current occurring at the moment t_0 and the decay of the ring current with the characteristic time τ_0. The b_{r0}, t_0, and τ_0 should be chosen in each disturbance proceeding from the observed Dst index profile by best fitting of it.

4. Results

All parameters of the model are determined from empirical data (solar wind parameters, AL, Dst, and the auroral electrojet maximum latitude). At each moment they represent an instantaneous state of the magnetosphere. The dynamics of the magnetosphere can be presented as a sequence of the instantaneous states.

Let us calculate the magnetic field on the Earth's surface using independent data of the magnetospheric disturbances of March 23–24, 1969 and July 24–26, 1986.

4.1. Magnetic Storm of March 23–24, 1969

Figure 1a shows King's catalogue data of the solar wind parameters in the interval March 23–24, 1969. These data allow calculation of the time dependence of the geocentric distance R_1 to the subsolar point based on [*Roelof and Sibeck*, 1993] results. The AL index shown in Figure 1b was determined by data of auroral and subauroral observations, taking into account expansion of the auroral electrojet during the magnetic storm [*Sumaruk et al.*, 1989]. The midnight location of westward electrojet maximum φ_k, (Figure 1c) is determined by using magnetometer chains data. This allows us to calculate the distance to the geotail current sheet earthward edge R_2.

In Figure 1d the Dst index is presented. It was constructed using the data of the 11 low-latitude stations for a magnetic storm of March 23–24, 1969 [*Sumaruk et al.*, 1989]. As one can see from Figure 1d, the Dst index profile has two minima. We explore two representations. The first corresponds to a single injection of particles where the ring current intensity was defined by formula (13). Using the minimum of the rms deviation of ΔB (see (2)) calculated on the Earth's equator from the Dst index (see Figure 1d), the injection beginning was chosen at $t_0 = 1800$ UT on March 23, the characteristic decay time was set to be $\tau_0 = 0700$ UT, and the maximum intensity of the ring current was chosen to be $b_{r0} = -200$ nT.

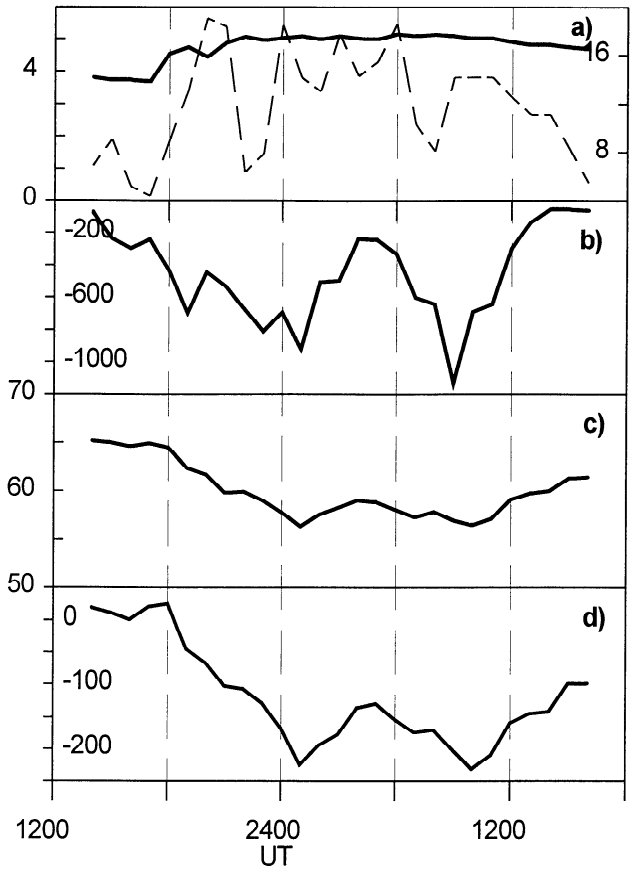

Figure 1. (a) Solar wind density (dashed line), in cm^{-3} (right scale), and velocity (solid line), in 100 km/s (left scale); (b) AL index, in nanoteslas; (c) latitude of the westward electrojet maximum, in degrees; and (d) Dst index, in nanoteslas, for the magnetic storm of March 23–24, 1969.

The second representation utilizes double injections. Since the profile of the Dst index had two distinct humps, formula (13) was used together with a version of two injections

$$b_r = b_{r1}\frac{t - t_1}{\tau_1}\exp\frac{\tau_1 + t_1 - t}{\tau_1}, \quad t_2 > t > t_1 \qquad (14a)$$

$$b_r = \sum_{i=1}^{2} b_{ri}\frac{t - t_i}{\tau_i}\exp\frac{\tau_i + t_i - t}{\tau_i} \quad t > t_2, \qquad (14b)$$

here sets (b_{r1}, t_1, τ_1) and (b_{r2}, t_2, τ_2) are determined similar to (b_{r0}, t_0, τ_0) in (13).

In (14), use was made of the values $t_1 = 1800$ UT on March 23, $t_2 = 0700$ UT on March 24, $\tau_1 = 0700$ UT, $\tau_2 = 0500$ UT, $b_{r1} = -180$ nT, and $b_{r2} = -70$ nT. As in the first case, b_r at the moment before t_1 was assumed to be zero. From t_1 until t_2, b_r was determined by the (14a), and at the moment later t_2, b_r was determined by the (14b).

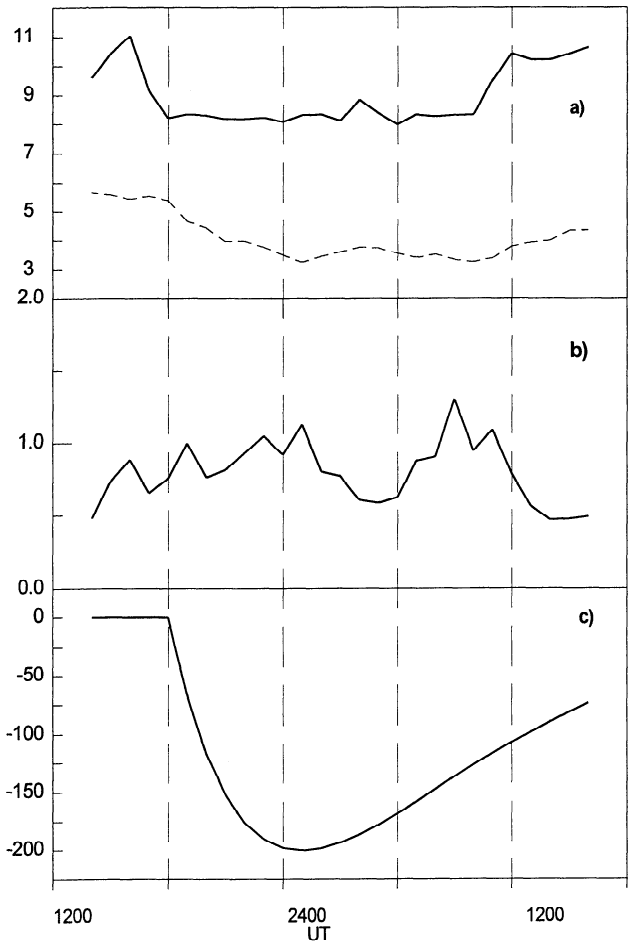

Figure 2. (a) The distances from the Earth's center to the subsolar point (R_1, solid line) and to the earthward edge of the geotail current sheet (R_2, dashed line), in R_E; (b) the magnetic flux through the geomagnetic tail lobe, in 10^9 Wb; and (c) the ring current intensity b_r, in nanoteslas, for the magnetic storm of March 23–24, 1969.

Thus it is possible to calculate (see sections 3.1–3.5) the time dependence of R_1, R_2, Φ_∞ and b_r for the interval under consideration (see Figures 2a, 2b, and 2c) and then to calculate the time dependence of the model field at the Earth's equator.

Figure 3a compares model calculations for the case of a single injection with the values of the Dst index. The dotted curve shows the field of the tail current system, the field of the ring current and of the magnetopause screening currents is depicted by the dashed curve, the solid curve presents a total modeled field of the magnetospheric sources (ΔB), and the thick solid curve is for measured values of the Dst index. The modeled fields of the last four terms in formula (1) were calculated at the Earth's equator and were multiplied by a factor of 1.5 because of the effect of interterrestrial induced currents preventing the external field penetration into the Earth [*Akasofu and Chapman,* 1972].

Figure 3b shows similar curves for the case of two injections. A comparison of Figures 3a and 3b shows that both "one-hump" and "two-hump" models give a good agreement with the observed values of the Dst index.

An examination of our results shows that modeling calculations reproduce onground measurements with an accuracy of tens of nanoteslas. Comparison of the Dst index, ΔB, and B_t time dependences shows that rapid changes of the Dst index are strongly correlated with the rapid changes of B_t. This agreement indicates that rapid variations of the Dst index are strongly influenced by spatial changes of the magnetospheric shape and by changes in the tail current system intensity (time dependence of the tail lobe magnetic flux).

Variations of the distance R_1 to the subsolar point (Figure 2a) reflect the effect of the solar wind dynamic parameters on the magnetospheric dimensions. Variations of R_2 (Figure 2a) are in a good accordance with the idea that the earthward edge of the geotail current sheet moves closer to the Earth as the activity ensues and moves downtail during the recovery phase. The calculated field magnitude at the inner edge of the tail current sheet ($b_t \lesssim 140$ nT) agrees with available data [*Kaufmann,* 1987; *Lui et al.,* 1992; *Lopez and von Rosenvinge,* 1993] during strong disturbances.

This analysis demonstrates that the magnetospheric tail current system makes a prominent contribution to the Dst index and is responsible for the fast changes of the Dst index.

4.2. Magnetic Disturbance of July 24–26, 1986

Figure 4 presents 1-hour values of solar wind and geomagnetic data during the period under consideration (solar

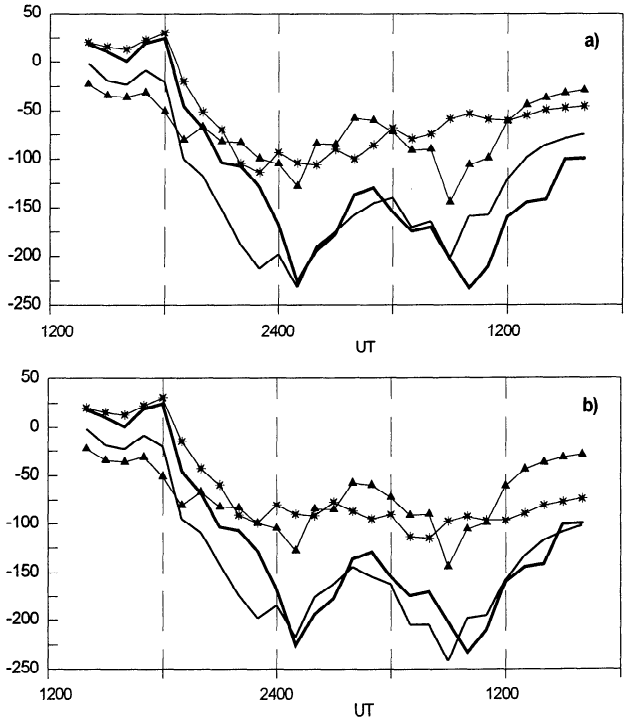

Figure 3. (a) The comparison of the Dst index (heavy solid line) and the modeled ΔB (solid line) for the magnetic storm of March 23–24, 1969 for the case of (a) one injection into the ring current and (b) two injections. The line marked by triangles is the contribution of geotail current system (B_t) to Dst, and the line marked by asterisks is the field of the ring current and Chapman-Ferraro currents (B_a).

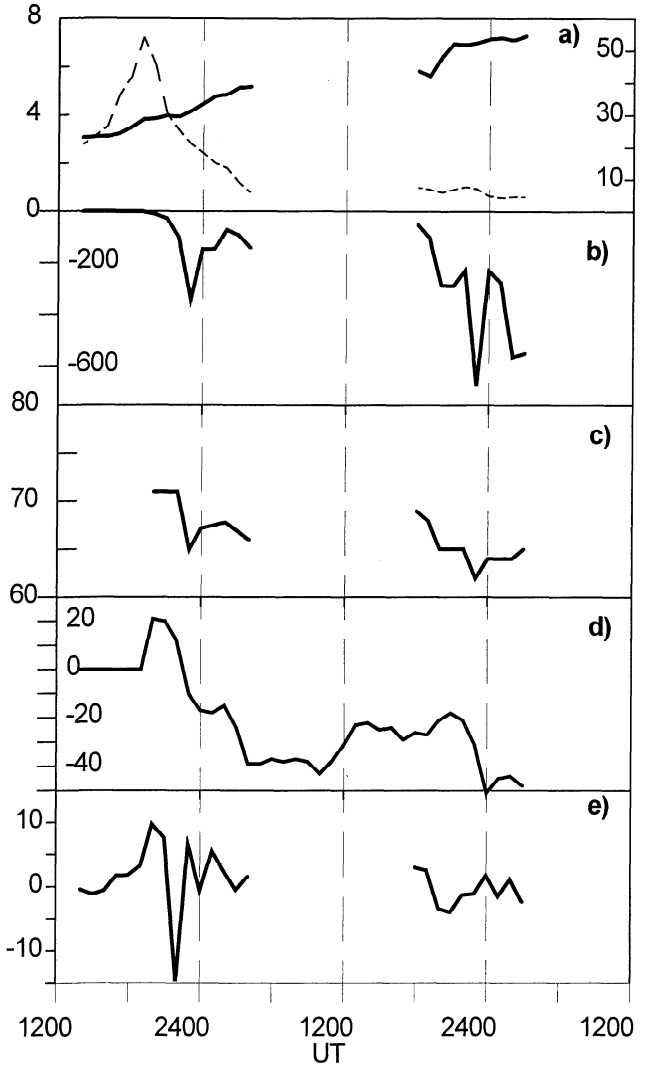

Figure 4. (a) Solar wind density (dashed line), in cm^{-3} (right scale), and velocity (solid line), in 100 km/s (left scale); (b) AL index, in nanoteslas; (c) latitude of the westward electrojet maximum, in degrees; (d) Dst index, in nanoteslas; and (e) B_z component of IMF, in nanoteslas, for the magnetic disturbance of July 24–26, 1986.

wind density and velocity (Figure 4a), AL index (Figure 4b), location of westward electrojet maximum (Figure 4c), Dst (Figure 4d), and B_z component of IMF (Figure 4e). The latitude of the electrojet maximum during disturbance is determined from the EISCAT magnetometer chain data presented by L. Hakkinen. The Dst index was determined using the data of the nine low-latitude stations. Unlike the strong magnetic storm of March 23–24, 1969 this disturbance was weak and was not accompanied by powerful particle injection from the geomagnetic tail into the ring current region.

During the interval 0500–1700 UT on July 25, 1986 there was a lack of the solar wind measurements, and model calculations were not carried out. Using the available data, the input parameters of the model were calculated by expressions (2)–(13).

Using the minimum of the rms deviation of the magnetic field calculated on the Earth's equator from Dst data (see Figure 4d), the injection beginning was chosen at $t_0 =$ 2200 UT on July 24, the characteristic decay time was set to be $\tau_0 = 1100$ UT, and the maximum intensity of the ring current was taken as $b_{r0} = -45$ nT.

In Figure 5 the modeled field is compared with the Dst index. As in Figure 3, the dotted curve shows the field of the tail current system; the dashed curve depicts the sum of the magnetic fields of the magnetopause screening currents and of the ring current; the solid curve presents the total modeled field of magnetospheric sources; and the thick solid curve represents measured values of the Dst index. The minimum of the Dst index near 2400 UT on July 24 is well described by the extremum of b_t, due to westward electrojet enhancement (see AL index in Figure 4c).

For independent checking of the model result we will study the auroral oval dynamic during this case. Approximating the polar cap by a circle with the center near the magnetic pole, we can express its magnetic flux as

$$\Phi_{pc} = 2B_0\pi R_E^2 \sin^2\theta_{pc}\,, \tag{15}$$

where B_0 is the magnetic field at the Earth's equator and θ_{pc} is the colatitude of the polar cap boundary. The polar cap flux Φ_{pc} is equal to the tail lobe flux Φ_∞. Using (7) we can estimate the polar cap scale:

$$\sin^2\theta_{pc} = \frac{1}{4}\frac{b_t R_1^2}{B_0 R_E^2}\sqrt{\frac{2R_2}{R_1}+1}\,. \tag{16}$$

Then we use the experimental data about the width of the nightside auroral oval and about location of the center of its equatorward boundary [see e.g., *Starkov and Feldstein*, 1967; *Iijima and Potemra*, 1976; *Holzworth and Meng*, 1984]. From these data and from the calculated radius of the polar cap the midnight latitudes of the auroral oval boundaries were determined.

In Figure 6 the latitudes of equatorward and poleward boundaries of the modeled auroral oval at 2400 magnetic local time and the westward electrojet maximum measured by EISCAT chain stations are presented. EISCAT data are in good accordance with the values of the equatorward boundary of the auroral oval, calculated by the magnetic flux variations through the geomagnetic tail.

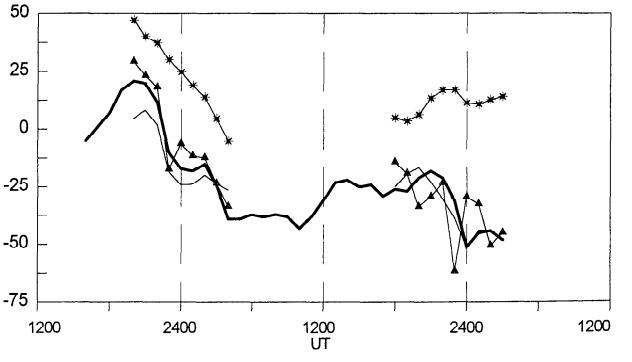

Figure 5. The comparison of the Dst index and the modeled ΔB for the magnetic disturbances of July 24–26, 1986. Notations are the same as in the Figure 3.

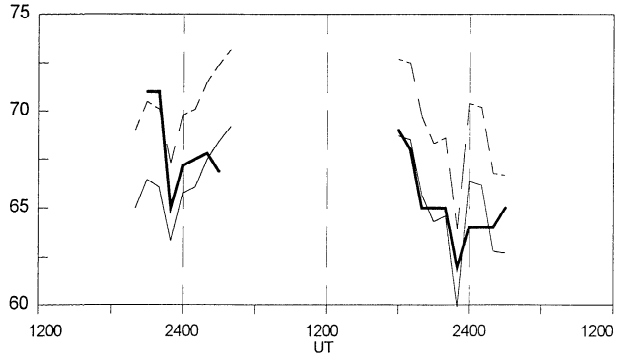

Figure 6. The auroral oval poleward (Fi_{po}, dashed line) and equatorward (Fi_{eq}, solid line) midnight latitudes calculated by model and the observed location of westward electrojet maximum (Fi, heavy solid line) during the interval of July 24–26, 1986.

The energy input rate into the magnetosphere can be evaluated using the parameter ε [*Perreault and Akasofu,* 1978]. The 1-hour values of ε are presented in Figure 7a for the interval under consideration. Two intense bursts at 2200 UT on July 24 and at 2100 UT on July 25 (see Figure 7a) correspond to the abrupt variations of the dynamic pressure of solar wind and of the IMF.

Total energy input to the magnetosphere is

$$E(t) = \int_{t_0}^{t} \varepsilon(t)\, dt\,, \tag{17}$$

where t_0 is the beginning of the disturbance (the same as in (13)).

The main part of this energy is deposited in the ionosphere and accumulated by geomagnetic tail current system [*Alexeev,* 1977; *Sergeev and Tsyganenko,* 1980]. The ionospheric Joule heating is

$$E_i(t) = \int_{t_0}^{t} Q_i(t)\, dt = \int_{t_0}^{t} I\, \Delta U\, dt\,, \tag{18}$$

and the tail storage of the energy is

$$E_t(t) = \Phi_\infty l_t \simeq 2\Phi_\infty b_t l_x/\mu_0\,, \tag{19}$$

where $Q_i = I\Delta U$ is Joule heating power, I is the total field-aligned current (assumed for simplicity to be 10^6 A), ΔU is the polar cap potential difference, l_x is the "geotail length", the distance from the earthward edge of the current sheet to the neutral line, calculated by *Alexeev et al.* [1989, 1993]. In Figure 7b the energy of Joule heating of the ionospheric current system (dotted line), the energy stored in the geomagnetic tail (dashed line), the sum of them (solid line), and the total energy $E(t)$ (see (17)) transported into the magnetosphere (thick solid line) are presented. The substorm energy changes are well described by the sum of the ionospheric Joule heating and geotail energy storage.

5. Discussion

The main finding of our paper concerns the contribution of the magnetic field of the cross-tail current to the Dst index during magnetic storms. We find that this contribution may be equal to or even more than the perturbation produced by the ring current. In checking this conclusion we will discuss several topics.

5.1. Verification of our Results

Two storms were studied in detail. One of them (March 23–24, 1969) has a large Dst index, with a maximum of $|D_{st}| \sim 200$ nT, and another one has a small Dst index. In each disturbance only three input parameters (t_0 is the moment of injection beginning, τ_0 represents the characteristic decay time of the ring current, and b_{r0} is the magnetic field corresponding to the current maximum during the disturbance) were chosen from the observed Dst index profile by best fitting. The other input model parameters were defined from independent experimental data. The hourly averaged strength of the magnetic field during about 48 hours was calculated. As a result, residual rms deviation of the model calculations from observational data is ~25 nT. The 10% accuracy is evidence of a good agreement between model calculations and observations.

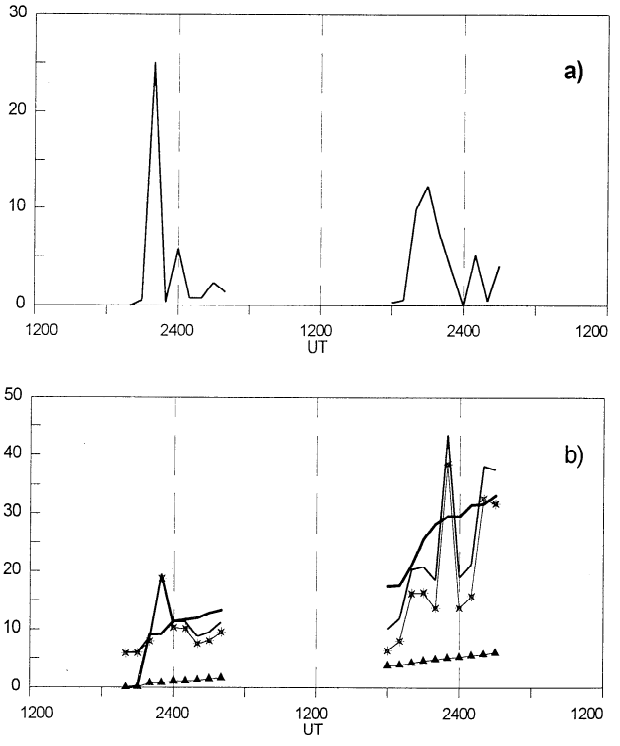

Figure 7. (a) The input power ε, in 10^{11} W, into the magnetosphere for the interval of July 24–26, 1986; (b) the energy of the ionospheric current system (line marked by triangles), the energy stored in the geomagnetic tail (line marked by asterisks), the sum of them (solid line), and the total energy transported into the magnetosphere $\int \varepsilon(t)dt$ (heavy solid line), in 10^{15} J, for the interval of July 24–26, 1986.

5.2. A Contribution from the Partial Ring Current

Fast (~1 hour) variations of the Dst index strongly support our conclusion of significant contribution of the tail current to the magnetic field variations. These variations can not be explained by variations of the symmetric ring current particle flux. However, partial ring current may have a similar timescale, and it is another possible cause of the Dst index fast variations [*Takahashi et al.,* 1991]. At first sight the partial ring current is very similar to the near-Earth cross-tail current. Both currents occupy the same region of the magnetosphere, at the distance of ~4–6 R_E in the nightside. However, they have different closure currents. The first (the partial ring current) is connected by field-aligned currents to the ionospheric currents, and the second (the cross-tail current) is closed by Chapman-Ferraro currents at the magnetopause. For this reason, the field of the total loop of the partial ring current has strong local time dependence at the Earth's equator, in contrast to the field of the cross-tail current system which is approximately independent of the longitude. It is easy to estimate from the Biot-Savart's law, that the longitudinal average of the partial ring current loop's field is ~20% of the amplitude of its asymmetric perturbation. The ratio of these terms (symmetric to the asymmetric) is roughly proportional to the ratio of the distance to the ionospheric part of the current loop R_E to the distance to the magnetospheric (equatorial) part of it R_{pr}. This ratio is about $R_E/R_{pr} \cong 0.2$, here $R_{pr} \sim 5\ R_E$ is the distance to the partial ring current.

We may estimate the contribution of the partial ring current to the Dst index during the storm of March 23–24, 1969, based on the measurements of the equatorial field asymmetry. These results were obtained by *Feldstein et al.* [1990] from the data of 11 magnetic low-latitude observatories. During the maximum of the main phase the asymmetric strength is ~100 nT and the maximal contribution from partial ring current to Dst index is ~20 nT. (It is about the accuracy of the model, see section 5.1.)

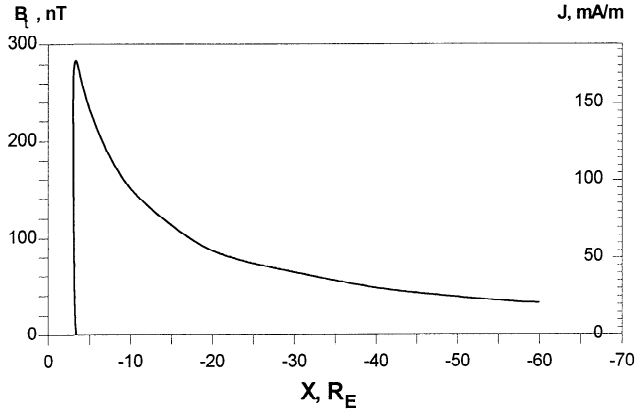

Figure 8. The x component of the tail magnetic field strength near to the current sheet, in nanoteslas (left scale), and the tail current density, in milliamperes per meter (right scale), are shown at the maximum of Dst during the March 24, 1969, storm. Both depend on the distance to the Earth r, as $1/r$. They are equal to zero closer than 3.5 R_E to the Earth.

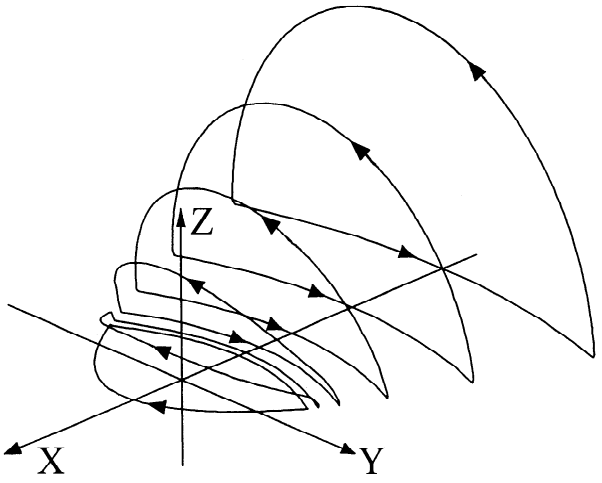

Figure 9. The current loops of the tail current system. One can see current sheet lines and closure return magnetopause current lines. The northern half of the magnetosphere is shown.

5.3. Unexpected Great Strength of Cross-Tail Current Field at the Earth's Equator

As one can see from Figure 3, sometimes the cross-tail current field may be as large as ~140 nT, in contrast to popular opinion that this value is about 20 nT [see e.g., *Tsyganenko and Sibeck,* 1994].

During the magnetic storm interval, the tail current strength increases. As shown in Figure 8, for the maximum of Dst (~0900 UT) in the March 24, 1969 storm the tail current density was about 300 mA/m at the inner edge of the current sheet (~3.5 R_E). This current density corresponds to the tail magnetic field strength of about 170 nT. In Figure 8 the model dependence of the tail field strength (as well as of the current density) on the distance along the Earth-Sun line is shown for moment of maximum of Dst. In Figure 8 only values of the x component of the tail field near to the equatorial plane are shown. It is zero closer to the Earth than to the inner edge of the current sheet.

The current increasing is one reason for the great strength of the cross-tail field, and the other reason is the peculiarity of the model three-dimensional current system connected with the tail currents. Our model of the tail currents is shown in Figure 9 [*Alexeev et al.,* 1975]. The closure currents are placed on the magnetopause starting from the subsolar point. The cross-tail currents together with the their magnetopause closure currents form the current loops which lie close to the equatorial plane. In the nearest to the Earth region of the magnetosphere their magnetic field structure is like the ring current's structure.

The cross-tail currents magnetic field lines connect northern and southern tail lobes through the inner magnetosphere equatorial cross section (from the dayside magnetopause to the inner edge of the geotail current sheet). For simple estimation of the average cross-tail current field at the Earth's equator one can use the ratio of the tail lobe magnetic flux to the area of the inner magnetosphere equatorial cross sec-

tion. During magnetic storms this area is reduced by about 2 times in comparison with the quiet conditions. This occurs because during magnetic storms the magnetopause is located closer to the Earth and the inner edge of the tail current sheet moves earthward. As one can see from Figure 2a, $R_1 \cong 8\,R_E$ and $R_2 \cong 4\,R_E$ during the studied case (average values $R_1 = 10\,R_E$ and $R_2 = 6\,R_E$).

On the other hand, the tail lobe magnetic flux may increase because of the solar wind pressure enhancement. The tail lobe magnetic field is balanced by the thermal pressure of the solar wind plasma. During the studied case (March 24, 1969) the solar wind plasma density increases by ~4 times. The tail lobe magnetic field strength must increase twice as $B_t \sim \sqrt{p}$. At the same time the lobe magnetic flux increases during magnetic storm. Owing to the rise of the tail lobe field strength and decrease of the equatorial section area, the cross-tail current field strength at geomagnetic equator increases by about 4 times in comparison with its quiet value. Taking into account the effect of interterrestrial induced currents preventing the external field penetration into the Earth [*Akasofu and Chapman,* 1972] (see section 4.1), we obtain the values of $B_t \simeq 120$ nT, closed to our model results.

5.4. Auroral Oval Size Modification Occurs During Magnetic Storms

There is numerous observational evidence [after *Akasofu and Chapman,* 1962; *Feldstein and Starkov,* 1968] that the nightside auroral oval latitude decreases with the Dst index increase. The hourly average location of the auroral oval's equatorward boundary moves to low latitude during magnetic storms. Auroral oval expansion is independent support of our conclusion about the key role of the cross-tail currents in the magnetospheric dynamics during magnetic storm. As was demonstrated by model calculations, the ring current may modify the polar cap and polar oval sizes only insignificantly. To the contrary, the cross-tail current directly controls the polar cap and auroral oval locations. This fact strongly supports our conclusion about the cross-tail current's contribution to the Dst index.

6. Conclusion

The magnetic field during magnetospheric disturbances is investigated using the dynamic model of the magnetosphere. The magnetic field changes with a characteristic time of about 1 hour are described as the corresponding variations of the parameters of large-scale current systems in the magnetosphere. The latter can be obtained using measured parameters of the solar wind (density and velocity) and of geomagnetic activity (the AL index, Dst, and the midnight latitude of an auroral electrojet maximum). The dynamic model enables us to describe the dynamics of the magnetospheric field during magnetic storm and high levels of auroral activity.

It was shown by model calculations of the ring current and tail current magnetic field during magnetic disturbances that the tail current magnetic field at Earth surface has approximately the same magnitude as the ring current magnetic field. As Figures 3 and 5 show, the conformity between the calculated and observed magnetic fields is rather good, especially during the recovery phase. It is important to note that the more rapid variations, that appear during the recovery phase, are caused by the tail current.

The fact that the tail current magnetic field supplies an important contribution to the Dst index is strongly supported by this investigation. In spite of the fact that measurements in a limited volume (at the Earth's surface) do not allow us to distinguish between two sources of the Dst index (ring current and geotail current), the time dependence of the disturbance and of the polar cap size suggests that our estimation of the tail current term in the Dst index is valid. As one can see, the polar cap size strongly related to Φ_∞ (see section 3.4), but the value of ring current does not influence the polar cap area. The good correspondence between model calculations of the auroral oval boundaries and EISCAT magnetometer chain measurements (see Figure 6) supports our conclusion.

Appendix

For calculating the magnetic flux (6) by using a paraboloid magnetospheric model, it is useful to deal with an orthogonal parabolic coordinate system, (α, β, φ). In terms of these coordinates the usual solar magnetospheric Cartesian coordinates are given by

$$\begin{aligned} x &= R_1(\beta^2 - \alpha^2 + 1)/2\,, \\ y &= R_1\alpha\beta\sin\varphi\,, \\ z &= R_1\alpha\beta\cos\varphi\,. \end{aligned} \tag{A1}$$

Here the constant α surfaces are confocal paraboloids of revolution that open toward the Sun (positive x), and the constant β surfaces are paraboloids with the same focus that open on the night side. The coordinate φ measures the angle around the Sun-Earth line, so the $\varphi = 0$ is the north and $\varphi = \pi/2$ lies on the duskside. The Earth is at the origin of solar-magnetospheric (SMG) coordinates and at $\alpha = 1$ and $\beta = 0$ in parabolic coordinates. The magnetopause is the $\beta = 1$ surface. The subsolar point on the magnetopause corresponds to $\alpha = 0$ and $\beta = 1$ or $(R_1, 0, 0)$ in SMG coordinates.

In (α, β, φ) coordinates the integral (6) is

$$\Phi_\infty = R_1^2 \lim_{\alpha\to\infty} \int_0^1 \alpha\beta\sqrt{\alpha^2+\beta^2}\,d\beta \int_{-\pi/2}^{\pi/2} B_{t\alpha}(\alpha,\beta,\varphi)\,d\varphi\,. \tag{A2}$$

For calculation of Φ_∞ we may take into account only the main term of the tail current field which decreases on the nightside more slowly. This term is [see *Alexeev et al.,* 1975]

$$B_{t\alpha} = b_t \frac{\alpha_0}{\alpha} \frac{1}{\sqrt{\alpha^2+\beta^2}}\,. \tag{A3}$$

The constant b_t is the tail current magnetic field strength at the earthward edge of the geotail current sheet, α_0 is determined by the distance to the earthward edge of the geotail current sheet:

$$R_2 = R_1(\alpha_0^2 - 1)/2. \quad \text{(A4)}$$

The other terms in the total field (1) decrease faster than the geotail field moving in antisunward direction. If the main term of B_t is proportional to $\sqrt{R_1/|x|}$, the other terms are proportional to $\exp(-|x|/R_1)$ [see *Alexeev*, 1978]. If we calculate (A2) using (A3), we will have (7):

$$\Phi_\infty = b_t \frac{\pi R_1^2}{2}\sqrt{\frac{2R_2}{R_1} + 1}. \quad \text{(A5)}$$

Acknowledgments. The authors thank Lasse Hakkinen, Finnish Meteorological Institute, Department of Geophysics, Helsinki Finland, for EISCAT magnetometer chain data.

This work was supported in part by the Deutsche Forschungsgemeinshaft with the project MASRAEL. YIF acknowledges the Russian Basic Research Foundation (RBRF) grant 93-05-8722, and the International Science Foundation (ISF) grant M6P000. Work at MSU was supported by RBRF grant 95-05-14057, and by ISF grants NCM000 and NCM300.

The Editor thanks W.D.Gonzales and Gordon Rostoker and a third referee for their assistance in evaluating this paper.

References

Akasofu, S.-I., and S. Chapman, Large-scale auroral motions and polar magnetic disturbances III, *J. Atmos. Terr. Phys., 24,* 785–796, 1962.

Akasofu, S.-I., and S. Chapman, *Solar-Terrestrial Physics,* Clarendon, Oxford, 1972.

Alexeev, I. I., Energy transfer during a magnetospheric substorms (in Russian), *Geomagn. Aeron., 17,* 885, 1977.

Alexeev, I. I., Regular magnetic field in the Earth's magnetosphere (in Russian), *Geomagn. Aeron., 18,* 656, 1978.

Alexeev, I. I., The penetration of interplanetary magnetic field into the magnetosphere, *J. Geomagn. Geoelectr., 38,* 1199, 1986.

Alexeev, I. I., A. A. Kirillov, and T. A. Chuykova, The current system in the magnetospheric tail (in Russian), *Geomagn. Aeron., 15,* 508, 1975.

Alexeev, I. I., E. S. Belenkaya, V. V. Kalegaev, and Yu. G. Lyutov, Electric field in the magnetospheric tail current sheet at southward IMF (in Russian), *Geomagn. Aeron., 29,* 896, 1989.

Alexeev, I. I., V. V. Kalegaev, and Ya. I. Feldstein, Modelling of the magnetic field in a strongly disturbed magnetosphere (in Russian), *Geomagn. Aeron., 32,* 8, 1992.

Alexeev, I. I., E. S. Belenkaya, V. V. Kalegaev, and Yu. G. Lyutov, Electric fields and field-aligned current generation in the magnetosphere, *J. Geophys. Res., 98,* 4041, 1993.

Aubry, M. P., C. T. Russell, and M. G. Kivelson, Inward motion of the magnetopause before a substorm, *J. Geophys. Res., 75,* 7018, 1970.

Eather, R. H., and R. L. Carovillano, The ring current as the source region for proton auroras, *Cosmic Electrodyn., 2,* 105, 1971.

Fairfield, D. H., Average and unusual location of the Earth's magnetopause and bow shock, *J. Geophys. Res., 76,* 6700, 1971.

Feldstein, Ya. I., Modelling of the magnetic field of magnetospheric ring current as a function of interplanetary medium parameters, *Space Sci. Rev., 59,* 83, 1992.

Feldstein, Ya. I., and G. V. Starkov, Auroral oval in the IGY and IQSY period and a ring current in the magnetosphere, *Planet. Space Sci., 16,* 129–133, 1968.

Feldstein, Ya.I., B. A. Belov, S. A. Golyshev, L. A. Dremukhina, L. A. Levitin, and P. V. Sumaruk, Magnetospheric activity during an intense magnetic storm on March 23–24, 1969 in connection with parameters of the interplanetary medium (in Russian), *Issled. Geomagn. Aeron. Fiz. Solntsa, 89,* 79, 1990.

Fok, M.-C., J. U. Kozyra, A. F. Nagy, C. E. Rasmussen, and G. V. Khazanov, Decay of equatorial ring current ions and associated aeronomical consequences, *J. Geophys. Res., 98,* 19,381, 1993.

Gonzalez, W. D., A. L. C. Gonzalez, L. C. Lee, and B. T. Tsurutani, Role of the lifetime of ring current particles on the solar wind - magnetosphere power transfer during the intense geomagnetic storm of 28 August 1978, *Planet. Space Sci., 38,* 765, 1990.

Gonzalez, W. D., J. A. Joselyn, Y. Kamide, H. W. Kroehl, G. Rostoker, B. T. Tsurutani, and V. M. Vasyliunas, What is a geomagnetic storm?, *J. Geophys. Res., 99,* 571, 1994.

Grafe, A., The influence of the recovery phase injection on the decay of the ring current, *Planet. Space Sci., 36,* 765, 1988.

Grafe, A., and A. Best, Bemerkungen zur Hypothese zweier Sturmzeitringströme, *Pure Appl. Geophys., 64,* 59, 1966.

Holzworth, R. H., and C.-I. Meng, Auroral boundary variations and the interplanetary magnetic field, *Planet. Space Sci., 32,* 25, 1984.

Iijima, T., and T. A. Potemra, The amplitude distribution of field-aligned currents at northern high latitude observed by Triad, *J. Geophys. Res., 81,* 2165, 1976.

Kaufmann, T. G. Substorm currents: Growth phase and onset, *J. Geophys. Res., 92,* 7471, 1987.

Kistler, L. M., F. M. Ipavich, D. C. Hamilton, G. Gloecker, B. Wilken, G. Kremser, and W. Stüdemann, Energy spectra of the major ion species in the ring current during geomagnetic storms, *J. Geophys. Res., 94,* 3579, 1989.

Kovner, M. S., and Y. I. Feldstein, Solar wind interaction with the Earth's magnetosphere, *Planet. Space Sci., 21,* 1191, 1973.

Lopez, R. E., T. von Rosenvinge, A statistical relationship between the geosynchronous magnetic field and substorm electrojet magnitude, *J. Geophys. Res., 98,* 3851, 1993.

Lui, A. T. Y., R. E. Lopez, B. J. Anderson, K. Takahashi, L. J. Zanetti, R. W. McEntire, T. A. Potemra, D. M. Klumpar, E. M. Greene, and R. Strangeway, Current disruptions in the near-Earth neutral sheet region, *J. Geophys. Res., 97,* 1461, 1992.

Maltsev, Yu. P., Relationship of *Dst*-variation to magnetospheric geometry (in Russian), *Geomagn. Aeron., 31,* 567, 1991.

Perreault, P., and S.-I. Akasofu, A study of geomagnetic storms, *Geophys. J. R. Astron. Soc., 54,* 547, 1978.

Pisarsky, V. Yu., N. M. Rudneva, Y. I. Feldstein, and A. Grafe, About the decay parameter of the ring current (in Russian), *Geomagn. Aeron., 26,* 454, 1986.

Pulkkinen, T. I., A study of magnetic field and current configuration in the magnetotail at the time of a substorm onset, *Planet. Space Sci., 39,* 833, 1991.

Pulkkinen, T. I., H. E. J. Koskinen, and R. J. Pellinen, Mapping of auroral arcs during substorm growth phase, *J. Geophys. Res., 96,* 21,087, 1991.

Roelof, E. C., and D. G. Sibeck, The magnetopause shape as a bivariate function of IMF B_z and solar wind dynamic pressure, *J. Geophys. Res., 98,* 21,421, 1993.

Rostoker, G., and S. Skone, Magnetic flux mapping consideration in the auroral oval and the Earth's magnetotail, *J. Geophys. Res., 98,* 1377, 1993.

Sergeev, V. A., and N.A. Tsyganenko, *The Earth's Magnetosphere* (in Russian), 174 pp., Nauka, Moscow, 1980.

Starkov, G. V., and Ya. I. Feldstein, Variations of auroral oval zone boundaries (in Russian), *Geomagn. Aeron., 7,* 62, 1967.

Stern, D. P., and I. I. Alexeev, Where do field lines go in the quiet magnetosphere, *Rev. Geophys., 26,* 782–791, 1988.

Sumaruk, P. V., Ya. I. Feldstein, and B. A. Belov, The dynamics of magnetospheric activity during an intensive magnetic storm (in Russian), *Geomagn. Aeron., 29,* 110, 1989.

Takahashi, S., M. Takeda, and Y. Yamada, Simulation of storm-time partial ring current system and the dawn-dusk asymmetry of geomagnetic variation, *Planet. Space Sci., 39,* 821, 1991.

Tinsley, B. A., and S.-I. Akasofu, A note on the lifetime of the ring current particles, *Planet. Space Sci., 30,* 733, 1982.

Tsyganenko, N. A., and D. S. Sibeck, Concerning flux erosion from the dayside magnetosphere, *J. Geophys. Res., 99,* 13,425, 1994.

Tsyganenko, N. A., and A. V. Usmanov, Determination of the magnetospheric current system parameters and development of experimental geomagnetic field models configuration of the geomagnetic tail during substorms, *Planet. Space Sci., 30,* 433, 1982.

I. I. Alexeev, E. S. Belenkaya, and V. V. Kalegaev, Institute of Nuclear Physics, Moscow State University, Moscow 119899, Russia. (e-mail: alexeev@dec1.npi.msu.su; elena@dec1.npi.msu.su; klg@dec1.npi.msu.su)

Y. I. Feldstein, Institute of Terrestrial Magnetism, Ionosphere and the Radiowave Propagation, Troitsk, Moscow Region, 142092, Russia.

A. Grafe, GeoResearch Center Potsdam, Adolf Schmidt Observatory, D-14823, Niemegk, Germany. (e-mail: grafe@gfz-potsdam.de)

(Received June 7, 1993; revised November 2, 1995;
accepted November 7, 1995.)